Explicit precipitation-type diagnosis from a model using a mixed-phase bulk cloud-precipitation microphysics parameterization

Stanley G. Benjamin, John M. Brown, and Tatiana G. Smirnova[1]

NOAA Earth System Research Laboratory

Boulder, CO

Submitted to ***Weather and Forecasting***
8 October 2015 – original version
Revised – 6 January 2016

Accepted for publication – 4 Feb 2016

* Corresponding author address: Stanley G. Benjamin, NOAA/ESRL, R/GSD1, 325 Broadway, Boulder, CO, 80305-3328; E-mail: Stan.Benjamin@noaa.gov

[1] Also affiliated with the Cooperative Institute for Research in Environmental Sciences, University of Colorado, Boulder, Colorado.

Abstract

The Rapid Refresh (RAP) and High-Resolution Rapid Refresh (HRRR), both operational at NOAA's National Centers for Environmental Prediction (NCEP) use the Thompson mixed-phase bulk cloud microphysics scheme. This scheme permits predicted surface precipitation to simultaneously consist of rain, snow and graupel at the same location under certain conditions. Here we describe the explicit precipitation-type diagnostic method used in conjunction with the Thompson scheme in the RAP and HRRR models. The post-processing logic combines the explicitly predicted multi-species hydrometeor data and other information from the model forecasts to produce fields of surface precipitation type that distinguish between rain and freezing rain, and to also portray areas of mixed precipitation. This explicit precipitation-type diagnostic method is used with the NOAA operational RAP and HRRR models. Verification from two winter seasons from 2013-2015 is provided against METAR surface observations. An example of this product from a January 2015 south-central United States winter storm is also shown.

1. Introduction

Diagnosis of precipitation type from weather forecast model predictions is important for public forecasting of winter storms, and also for air and surface transportation, energy, hydrology, and other applications. The advent of mixed-phase bulk microphysics schemes in some NOAA operational numerical prediction models (Rapid Update Cycle, RUC – Benjamin et al., 2004a,b, Rapid Refresh, RAP – Benjamin et al. 2016, HRRR – Alexander et al. 2016) enabled a relatively direct diagnosis of precipitation type (e.g., rain, snow, ice pellets (IP), freezing rain and drizzle (FZ), mixed types) at the surface. Since 1998, the RUC model running at NOAA National Centers for Environmental Prediction (NCEP) has used a bulk scheme in which separate mixing ratios for cloud water, rain water, ice, snow and graupel are predicted at each 3-d grid point. From 2005-2012, the scheme used in RUC was as described by Thompson et al. (2004). The RAP, which replaced the RUC at NCEP on 1 May 2012, uses a more advanced version (Thompson et al. 2008). RAP version 3 and HRRR version 2, implemented at NCEP in 2015 (Benjamin et al. 2016), use an aerosol-aware version of the Thompson scheme (Thompson and Eidhammer 2014). This use of multi-species mixed-phase microphysics in the RUC, RAP and HRRR models was motivated by a need to improve forecast skill for clouds in general, and supercooled liquid water in particular, for aviation requirements. Here, we describe the diagnostic precipitation-type (p-type) scheme used in the NCEP RAP version 3 and HRRR version 2 (Alexander et al. 2016) as of late 2015.

63 This p-type scheme is a recent alternative to profile-based diagnostic methods
64 summarized in Section 2. Ikeda et al. (2013) presented verification results on p-
65 type forecasts from an earlier version of HRRR as of 2012. This paper is an
66 expansion and correction on their Table 1 and includes an examination of more
67 recent explicit p-type results.
68
69 The RAP and HRRR models use the community NCEP Unified Post-Processor
70 (UPP) also used for other models. Options have been added to UPP including
71 ceiling (cloud base height), visibility, and p-type, designed for microphysics
72 schemes with multiple prognostic hydrometeor-species variables. In this paper,
73 we describe the UPP option for this explicit, multi-species diagnostic of p-type,
74 currently applied only in the RAP and HRRR.
75

76 2. Other precipitation-type diagnostic schemes

77 Well before the introduction of mixed-phase microphysics schemes into some
78 operational numerical weather prediction models, successful diagnostic
79 techniques were designed using implicit assumptions about microphysical
80 processes to allow estimate of p-type. These procedures can be grouped into: 1)
81 algorithmic or decision-tree approaches based on an observed or predicted
82 sounding; and 2) statistical procedures that make use of a training dataset to
83 derive a set of equations that is then applied to predicted fields. All of the
84 diagnostic schemes discussed here are for discrete yes/no identification of each

85 p-type, the same yes or no designation in observer guidelines in the NOAA
86 Federal Meteorological Handbook No. 1 (OFCM, 2005, Chapter 8).
87
88 *a. Algorithmic approaches*
89 A number of simple but effective algorithms have been developed that use as
90 input model-forecast profiles of temperature and relative humidity from the
91 surface upward to the level of assumed precipitation-generating layers aloft. The
92 algorithms used most often by forecasters in North America are those developed
93 by Ramer (1993) and Baldwin et al. (1994). A description of Ramer's algorithm
94 can be found in Bourgouin (2000), Wandishin et al. (2005) and DeGaetano et al.
95 (2008). (The latter paper introduces some modifications to Ramer for application
96 to forecasts of ice accretion.) In essence, Ramer's approach is to define an ice
97 fraction of the precipitation in a precipitation-generation layer and, based on the
98 temperature of that layer, assume the ice fraction of this precipitation is either 0
99 (liquid) or 1 (frozen). Then, for the frozen case, a decision tree that depends on
100 the wet-bulb temperature profile is used to modify the ice fraction as a function of
101 height between the base of the generating layer and the ground. The value of
102 the ice fraction then determines p-type.
103
104 The Baldwin et al. algorithm also considers the vertical profile of wet-bulb
105 temperature below saturated layers where precipitation is presumed to form. If
106 this precipitation is presumed frozen, the p-type at the surface is obtained by

using the vertically integrated departure of the wet-bulb temperature from 0°C in various layers and the temperature in the lowest model layer. A more complete description can be found in Bourgouin (2000) and Wandishin et al (2005).

b. Statistical approaches

Among statistical approaches of which we are aware, the earliest to use upper-air data is that of Wagner (1957). Using surface aviation observations of precipitation type and collocated rawinsonde observations (about 40 stations), Wagner compared the thickness of the 1000-500-hPa layer to the occurrence of frozen precipitation and determined the thickness values corresponding to a 50% probability of frozen precipitation. The thickness values so obtained are still used by many forecasters as a point of comparison with predicted thickness values.

The Model Output Statistics (MOS) approach for p-type was first applied by Bocchieri (1979, 1980) and Bocchieri and Maglaras (1983) to the then-operational Limited-area Fine Mesh (LFM) model. Since then, there have been many upgrades, and MOS is now applied to output from the Global Forecast System (GFS) as well as the North American Mesoscale (NAM) models for precipitation type purposes. Perfect-prog (Vislocky and Young 1989) approaches include Keeter and Cline (1991) and Bourgouin (2000). Keeter and Cline use radiosonde 1000–700-, 1000–850- and 850–700-hPa thickness values at Raleigh-Durham, NC regressed against co-located surface observations. The

129 approach of Bourgouin (2000) classifies sounding temperature profiles into 4
130 groupings (freezing rain or ice pellets, ice pellets or rain, snow or rain, and snow)
131 and derives statistics separately for each grouping. Separate positive and
132 negative areas on a thermodynamic diagram between the 0°C isotherm and the
133 observed temperature profile are computed for each sounding in the training
134 dataset and are determined to be important predictors. Bourgouin considers his
135 approach most applicable to synoptic situations characterized by broad synoptic-
136 scale lift leading to widespread, deep saturation. Manikin (2005) combined the
137 Baldwin, Ramer, Bourgouin, and revised Baldwin algorithms into a single
138 predominant p-type value now used often in NCEP models
139 (http://www.wpc.ncep.noaa.gov/wwd/impactgraphics/).
140
141 A recent contribution by Schuur et al. (2012) shares conceptual aspects with the
142 earlier algorithmic approaches as well as that of Bourgouin in that it classifies
143 vertical profiles (model or observed) according to the number of 0°C crossings by
144 the wet-bulb vertical temperature profile together with the 2-m temperature. It
145 considers local extrema of this profile between the intermediate 0°C crossings.
146 This algorithmic approach could stand alone, but is intended for use in
147 conjunction with polarimetric radar, in which the radar polarimetric parameters
148 indicate whether a bright band (i.e., a melting layer) exists. If such a layer is
149 detected, then precipitation type at the ground is expected to be rain, freezing
150 rain, ice pellets or a mixture of freezing rain and ice pellets, or possibly even wet

151 (melting) snow if the melting level is detected at the lowest elevation scan, but
152 not dry snow.
153
154 ## 3. Explicit diagnostic scheme for precipitation type
155 In the post-processing algorithm described here, separate yes/no indicators are
156 diagnosed for each of 4 different p-type categories: rain, snow, ice pellets
157 (including graupel) and freezing rain. These yes/no indicators are determined
158 from the explicit 3-d hydrometeor mixing ratios reaching the ground calculated in
159 the cloud microphysics parameterization (Thompson et al. 2008, Thompson and
160 Eidhammer 2014) in the RAP or HRRR models (or from the Thompson et al.
161 2004 scheme in the RUC model). The hydrometeor fields predicted by the
162 Thompson schemes are mixing ratios of cloud water (droplets), rain, cloud ice,
163 snow and graupel, as well as number concentration of raindrops and cloud-ice
164 particles.[2] These hydrometeor mixing ratio prognostic fields undergo horizontal
165 transport as well as vertical transport at appropriate fall speeds. The p-type
166 diagnostic algorithm described here makes use of the explicit precipitation of
167 rain, snow and graupel predicted to reach the surface by the model. Using
168 continuous model-provided explicit fields of hydrometeor mixing ratios and fall
169 rates (mass accumulation at ground per unit time), this algorithm estimates
170 thresholds for these parameters to approximate the same discrete yes/no

[2] The number concentration of cloud water drops is also predicted in the Thompson-Eidhammer aerosol-aware scheme but is not used in the precipitation identification described here.

observer guidelines in the NOAA Federal Meteorological Handbook No. 1 (OFCM, 2005, Chapter 8).

The explicit p-type scheme described here depends on the microphysics scheme to provide a "first guess" of precipitation types reaching the ground. (Note that because rain, snow and graupel are each predicted separately by the forecast model, i.e., each possessing separate mixing ratios and fall speeds, it is possible for the model to predict that two or more of these will reach a given point on the ground simultaneously.) For each allowable p-type in this diagnostic scheme (rain, snow, ice pellets, freezing rain), the model output within each grid column (not just at the surface) is used to derive a separate yes/no (1/0) decision on whether that type is reaching the ground. These p-type values from the post-processing are not mutually exclusive, except for rain vs. freezing rain. More than one value (as many as three) can be yes (1) at a given grid point at a given time.

a. Diagnostic logic flowchart for precipitation types

The sequence of the diagnostic logic is depicted completely in the flowchart in Fig. 1, with further discussion below. The rationale for this scheme is provided in the following subsection. Each model grid column is considered separately, and all precipitation rates below are at the ground and in liquid-water equivalent. After determining if there was even a minimal amount of precipitation during the last hour (including that from parameterized convection, if appropriate, using 0°C

193 as a snow/rain threshold), the explicit p-type diagnosis logic is treated for 3
194 decisions: rain vs. freezing rain/drizzle, snow vs. rain, and ice pellets vs. rain or
195 snow. Each treatment allows consideration of instantaneous precipitation (via fall
196 rates for rain, snow, or graupel) and precipitation over last hour.
197
198 Some of the p-type rules are based on a *snow fraction (SF)* defined as mass of
199 snow accumulation divided by combined mass of snow and rain. *SF* is
200 calculated at each grid point for accumulation over some previous forecast
201 period. These precipitation accumulations are updated each time step from the
202 near-surface mixing ratio times the fall speed, as described in Thompson et al
203 (2008) and Thompson and Eidhammer (2014). In the RAP and HRRR, the
204 previous forecast period is currently 1 h but can be set to shorter time periods
205 (e.g., 15 min).
206
207 1) Snow vs. rain
208 If *SF* > 0.25 *and* either current snow precipitation rate > 0.00072 mm/h (0.2 x
209 10^{-9} m s^{-1}) (liquid equivalent) *or* total precipitation of rain plus snow during the
210 previous hour > 0.01 mm, snow is diagnosed as long as current 2-m
211 temperature (from the model forecast) < 3°C. If 2-m temperature ≥ 3°C, rain is
212 diagnosed instead.
213 2) Rain vs. freezing rain (FZ)

214 If *SF* < 0.6 and either the current rain rate at ground is at least 0.01 mm/h or
215 there has been at least 0.01 mm total precipitation of rain plus snow during the
216 previous hour, then rain or freezing rain is diagnosed. If the 2-m temperature <
217 0°C, freezing rain/drizzle is diagnosed; otherwise, rain is diagnosed.
218 3) Ice pellets and related dependencies
219 Dependencies regarding IP diagnosis are more complicated out of the attempt
220 to match observing guidelines as described earlier in section 3. If current fall
221 rate for graupel > 0.0036 mm/h (1.0×10^{-9} ms^{-1}), ice pellet (IP) precipitation is
222 generally diagnosed, but with further dependencies including 2-m temperature
223 and relative instantaneous fall rates for graupel, rain, and snow. First, for IP,
224 the graupel fall rate at the surface must be greater than that for snow;
225 otherwise, S is diagnosed and not IP. Also to limit IP diagnosis to situations
226 with conditions normally expected, there must be a level aloft with rain mixing
227 ratio > 0.005 g kg^{-1}. (Note: With a previous maximum rain mixing ratio set as
228 > 0.05 g kg, IP was rarely diagnosed (Elmore et al. 2014), resulting in this
229 modification.) If, in addition, the fall rate for graupel is greater than that for rain,
230 IP **only** is diagnosed, not FZ and not rain. If 2-m temperature > 3°C, IP is not
231 diagnosed, thus not allowing IP to include the condition of convectively
232 produced hail.
233
234 *b. Rationale for explicit precipitation type diagnosis*
235 Although the model generally produces a dominant p-type, in the difficult cases
236 of cold-season mixed precipitation, simply using the p-types directly from the

model without any qualification as to the surface accumulation rate of that particular species leads to a confusing picture when displayed as a superposition of binary (0/1) fields. This is because at 2-m temperatures not far from 0°C, the physical solution within a multi-species microphysics scheme can give small amounts of more than one hydrometeor species falling to the surface in the model. Thus, it was necessary to introduce post-processing logic into the classification scheme for appropriate thresholds of multi-species fall rate.

Thresholds for *SF* and 2-m temperature in the p-type diagnostic logic were subjectively estimated (no effect on the actual forecast model solution) against observations of precipitation type from ASOS (Automated Surface Observing System) reports to avoid the problem of diagnosing too large (or too small) areal coverage of mixed precipitation (e.g., rain/snow or freezing rain/ice pellets/snow). It is also necessary to make use of the model forecast of 2m temperature to identify situations where rain is falling at temperatures < 0°C, and to limit IP diagnosis to formation in cold-season storms and exclude convectively produced hail. Allowing snow p-type identification with 2-m temperature up to 1°C accounts for wet-bulb effect, which is already identified in the Thompson microphysics via energy exchange between snow and environmental air as the snow falls at its fall speed.

259 In order to increase the likelihood of successfully predicting freezing drizzle at
260 the surface, the more recent Thompson microphysics schemes (Thompson et
261 al. 2008, Thompson and Eidhammer 2014) include a two-moment rain
262 component in order to better describe the collision-coalescence process in
263 clouds that are mainly composed of liquid particles but at temperature < 0°C
264 throughout the cloud depth.
265
266 We also note that the precipitation rates used currently for the model explicit p-
267 type diagnosis are 1) instantaneous, and 2) have a minimum threshold (0.0001
268 mm/h) much lighter than sensible by current measurement methods. The use
269 of the instantaneous precipitation rates means that this diagnostic method
270 could be expanded into higher frequency products or into a future PDF p-type
271 field. The very small precipitation rate thresholds were designed to capture
272 very light drizzle or light snow events, even at the expense of showing a bias
273 vs. ASOS-level-sensitivity for precipitation types (not shown). Thériaux et al
274 (2006) and Thériaux and Stewart (2010) considered a p-type fraction but did
275 not address how to approximate observer guidelines for yes/no p-type
276 identification.
277
278 **4. Case study and 2015 validation**
279 *a. Case example*

280 A brief example is shown to illustrate application of the explicit p-type diagnosis
281 in Figs. 2-4 for a winter storm forecast valid at 1600 UTC 1 January 2015.
282 Figure 2(a,b) shows p-type diagnosed from a RAP (13 km) 1-h forecast with
283 areas of snow (S), freezing rain, and ice pellets from New Mexico across
284 northern Texas with rain over southern Texas. Smaller areas of mixed
285 precipitation types are shown over northern Texas to the Arkansas-Louisiana
286 border in the 1-h forecast with the explicit p-type diagnosis, including S-FZ, FZ-
287 IP and R-IP mixtures. The total 1-h precipitation is added in Fig. 2b, indicating
288 the superset of possible areas for p-type assignment (gray) and areas of
289 heavier precipitation (>0.1 in/h in light green), usually for rain but some for FZ
290 and IP. A breakdown of each p-type forecast area is added in Fig. 3 to see the
291 specific coverage areas of each p-type. The METAR (Meteorological
292 Aerodrome Report) observations of p-type valid at the forecast valid time are
293 shown in Fig. 4. Freezing rain observations in Fig. 4 are generally within the
294 FZ forecast area evident in Figs. 2 and 3. The rain-snow line in observations
295 (Fig. 4) is very close to that diagnosed for the 1-h RAP forecast. Some snow
296 and FZ reports are shown in the Dallas-Fort Worth area (Fig. 4), similar to the
297 mixed S-FZ area forecast just west of those cities. A freezing rain report (Fig.
298 4) at 1500 UTC in central Texas (Abilene) was covered by the forecast FZ area
299 in Figs. 2 and 3. FZ was diagnosed near but not covering the Lubbock FZ
300 report in western Texas. The areal coverage in the forecast, especially for
301 snow and freezing rain, is larger than shown in observations, due to the very

light precipitation threshold of 0.0001 mm/h, well below the measurable minimum of about 0.25 mm/h. Areas of 1-h precipitation (supersets of the areas of instantaneous precipitation) are also shown for rain, snow, and graupel in Fig. 5, the starting point for the algorithm. The value added of applying the explicit p-type algorithm can be seen in comparing Fig. 5 with Fig. 3 (and in Fig. 2b). The p-type algorithm identifies areas of ZR and limits R, S, and IP assignment by the temperature, precipitation intensity, and other constraints shown in the logic flow in Fig. 1 and described in Section 3.

For comparison with another p-type diagnostic, Fig. 6 shows the results from the dominant p-type (Manikin 2005) combining Baldwin, Ramer, Bourgouin, and revised Baldwin techniques using gridded data from the same RAP 1h forecast shown in Fig. 2 and 3 for the explicit p-type diagnostic described in this paper. The general coverage is slightly larger with the dominant p-type in Fig. 6 (any precipitation greater than zero qualifies). The dominant p-type (Fig. 6) also shows a significant area of ice pellets in western Texas not shown with the explicit p-type diagnosis. A sounding for Lubbock, TX (Fig. 7) from the same common RAP 1-h forecast grid used for both p-type diagnoses indicates a saturated level above 0°C that could support IP, although the explicit p-type based on Thompson microphysics indicated snow with occasional mixed ZR. Observations from 1400-1900 UTC showed only ZR and S observations in western Texas (only 1600 UTC shown in Fig. 4).

Generally fewer details are shown in Fig. 6 (dominant) than Fig. 2 (explicit), including the freezing rain in western Texas and snow reports near the Dallas area. The dominant p-type scheme also cannot show mixed precipitation, by definition, but this condition is diagnosed with the explicit p-type scheme in Fig. 2 in some areas in northern Texas. This comparison is qualitative and suggests that the explicit p-type diagnosis is credible.

b. Validation of explicit 1h p-type forecasts from HRRR and RAP

Probability of detection for 1h RAP (ESRL experimental) p-type forecasts is presented in Fig. 8 over a 24-month period including two winter seasons using the nearest 13-km RAP grid point to METAR observation location. The probability of detection for occurrence events (PODy) is ~0.9 in all of the 24 months over the conterminous US for rain and about 0.8-0.9 for snow over the same period during winter months. PODy for IP ranges from 0.3 to 0.55 (most common month- February) and slightly lower for FZ. The PODy for IP from this diagnostic is far higher than that shown in Elmore et al. (2015) who used RAP results not including the IP algorithm change in the ESRL version in January 2013. Both IP and FZ usually occur in geographically limited areas, so high PODy is difficult to achieve in real-data modeling. The deficiency in PODy for IP and FZ is likely due to errors in temperature, water vapor, and hydrometeor initialization. The number of IP and FZ events are rare: for instance, during February 2015, for METARs within the CONUS area including

346 southern Canada, the total number of reports was about 60,000 for snow,
347 30,000 for rain, 2000 for freezing drizzle/rain, and 400 for ice pellets. As
348 mentioned at the end of section 3, the p-type diagnostic method uses a
349 minimum threshold (0.0001 mm/h) much lighter than sensible by current
350 measurement methods (minimum 0.25 mm/h), resulting in a high False Alarm
351 Ratio (FAR) vs. METAR observations (Fig. 9).[3] The overall FAR for
352 measurable (0.25 mm) precipitation for RAP vs. METARs is depicted in Fig.
353 10, showing an overall FAR of about 0.35-0.40, much lower than that shown in
354 Fig. 9 with the far lower threshold for the p-type algorithm designed to capture
355 very light but significant freezing precipitation events.

356 **5. Conclusions**

357 The explicit p-type diagnostic scheme described here is a relatively new
358 approach applicable with explicit model forecasts of rain, snow, and graupel
359 precipitation at the surface. This scheme has been applied to NOAA
360 operational models that use the Thompson cloud and precipitation
361 microphysics, specifically, the HRRR and RAP, and before 2012, with the
362 RUC. This scheme was shown to provide effective results in a 2-year

[3] It should be noted that the Automated Surface Observation System (ASOS) used at METAR sites currently does not have the ability to detect IP. This precipitation type is nominally only reported when an ASOS observation is augmented by a human observer, partially accounting for the paucity of IP reports.

363 evaluation and in a winter storm case study. This scheme has been used at
364 NCEP in its hourly updated models (RUC, RAP, HRRR) since 2005. [4]
365
366 This explicit diagnosis of p-type from the RAP and HRRR is directly linked with
367 the multi-species cloud microphysics. Uncertainty in forecast thermodynamic
368 structure is obviously a source of error in p-type forecasts using this diagnostic
369 method, as shown for other methods (Thériaux et al. 2006, Reeves et al.
370 2014). Probabilistic p-type forecasts are an obvious extension of this explicit p-
371 type algorithm, using time-lagged and explicit ensembles of RAP, HRRR
372 and/or other models with multi-species cloud microphysics schemes. Explicit
373 p-type forecasting accuracy is expected to further improve with assimilation of
374 dual-polarization radar with diagnostic of hydrometeor type, a direction being
375 taken in RAP and HRRR data assimilation development.
376
377 It should be noted that the algorithm discussed here is intended for wintertime
378 application. The Thompson microphysics scheme (both the 2008 and 2014
379 versions) does not have a separate hail category but, in situations conducive to
380 deep convection, will sometimes produce graupel precipitation during the warm
381 season when used within cloud permitting forecast models such as the HRRR.

[4] Occurrence of mixed snow/rain was excessively diagnosed with this scheme until a correction to a snow fraction error in January 2011. The scheme as described here, including the January 2011 correction also noted in Ikeda et al (2013), was incorporated into the initial implementation of the RAP at NCEP on 1 May 2012.

382 Work to introduce a hail-size algorithm into the Thompson microphysics for
383 warm-season forecast applications will be discussed elsewhere.
384
385 ACKNOWLEDGMENTS
386
387 We thank Joseph Koval at The Weather Company and Kyoko Ikeda and her
388 NCAR colleagues for their help in identifying problems with the RUC precipitation
389 type that led to improvements in the scheme now documented in this note. We
390 also thank Greg Thompson at the National Center for Atmospheric Research for
391 ongoing collaboration, and colleagues at NOAA/ESRL especially Curtis
392 Alexander and Brian Jamison for their help on evaluation of the p-type algorithm
393 described here. We thank Kim Elmore and his colleagues at NSSL for
394 prompting identification of need for the IP criterion resetting. Ongoing changes
395 in the p-type diagnostic described in this paper are tracked under
396 http://ruc.noaa.gov/rr/RAP_var_diagnosis.html#ptype. Finally, we thank Trevor
397 Alcott, David Dowell and John Osborn (NOAA/ESRL) for very helpful reviews.
398 The Federal Aviation Administration has partially supported some of this work.
399
400 REFERENCES
401
402 Alexander, C.A., D.C. Dowell, S.G. Benjamin, S.S. Weygandt, M. Hu, E. James,
403 J.M. Brown, J.B. Olson, and T.G. Smirnova, 2016. The High-Resolution

Rapid Refresh, an hourly updated storm-resolving model. Manuscript in preparation.

Baldwin, M., R. Treadon and S. Contorno, 1994: Precipitation type prediction using a decision tree approach with NMC's Mesoscale Eta Model. *Preprints, Tenth Conf. on Numerical Weather Prediction*, American Meteorological Society, Portland OR, 30-31.

Benjamin, S.G., G. A. Grell, J. M. Brown, and T. G. Smirnova, 2004a: Mesoscale weather prediction with the RUC hybrid isentropic-terrain-following coordinate model. *Mon. Wea. Rev.*, **132**, 473-494.

Benjamin, S.G., D. Devenyi, S.S. Weygandt, K.J. Brundage, J.M. Brown, G.A. Grell, D. Kim, B.E. Schwartz, T.G. Smirnova., and T.L. Smith, 2004b: An hourly assimilation-forecast cycle: the RUC. *Mon. Wea. Rev.*, **132**, 495-518.

Benjamin, S. G., S.S. Weygandt, M. Hu, C.A. Alexander, T.G. Smirnova, J.B. Olson, J.M. Brown, E. James, D.C. Dowell, G.A. Grell, H. Lin, S.E. Peckham, T.L. Smith, W.R. Moninger, J. Kenyon, G.S. Manikin, 2016, A North American hourly assimilation and model forecast cycle: The Rapid Refresh. *Mon. Wea. Rev.*, doi: http://dx.doi.org/10.1175/MWR-D-15-0242.1

Bocchieri, J.R., 1979: A new operational system for forecasting precipitation type. *Mon. Wea. Rev.*, **107**, 637-649.

Bocchieri, J.R., 1980: The objective use of upper air soundings to specify

precipitation type. *Mon. Wea. Rev.*, **108**, 596-603.

Bocchieri, J.R., and G.J. Maglaras, 1983: An Improved operational system for forecasting precipitation type**.** *Mon. Wea. Rev.,* **111**, 405-419.

Bourgouin, P., 2000: A method to determine precipitation types. *Wea. Forecasting*, **15**, 583-592.

DeGaetano, A. T., B. N. Belcher, and P. L. Spier, 2008: Short-term ice accretion forecasts for electric utilities using the Weather Research and Forecasting model and a modified precipitation-type algorithm. *Wea. Forecasting***, 23**, 838-853.

Elmore, K.L., H.M. Grams, D. Apps, H.D. Reeves, 2015, Verifying forecast precipitation type with mPING. *Wea. Forecasting,* **30**, 656-667. doi: http://dx.doi.org/10.1175/WAF-D-14-00068.1

Ikeda, K., M. Steiner, J. Pinto, C.A. Alexander, 2013: Evaluation of cold-season precipitation forecasts generated by the hourly-updating High-Resolution Rapid Refresh model. *Wea. Forecasting*, **28**, 921-939. doi: http://dx.doi.org/10.1175/WAF-D-12-00085.1

Keeter, K.K., and J.W. Cline: 1991: The objective use of observed and forecast thickness values to predict precipitation type in North Carolina. *Wea. Forecasting,* **6**, 456-469.

Manikin, G. S., 2005: An overview of precipitation type forecasting using NAM and SREF data. Preprints, *21st Conf. on Wea. Analysis & Forecasting / 17th Conf. on Numerical Weather Prediction,* Washington, DC, Amer.

448 Meteor. Soc., 8A.6.
449 Office of Federal Coordinator for Meteorology, 2005: Federal Meteorological
450 Handbook No. 1 - Surface Weather Observations and Reports. Available
451 at http://www.ofcm.gov/fmh-1/fmh1.htm
452 Ramer, J., 1993: An empirical technique for diagnosing precipitation type from
453 model output. Preprints, *5th Conf. on Avia. Wea. Systems*, Vienna, VA,
454 Amer. Meteor. Soc., 227-230.
455 Reeves, H.D., K.L. Elmore, A. Ryzhkov, T. Schuur, J. Krause, 2014: Sources of
456 uncertainty in precipitation-type forecasting. *Wea. Forecasting*, **29**, 936-
457 953.
458 Schuur, T. J., H.-S. Park, A. V. Ryzhkov, and H. D. Reeves, 2012: Classification
459 of precipitation types during transitional winter weather using the RUC
460 model and polarimetric radar retrievals. *J. Appl. Meteor. Clim.*, **51**, 763-
461 779. doi: http:// dx.doi.org/10.1175/JAMC-D-11-091.1
462 Thériaux, J.M., R.E. Stewart, and W. Henson, 2006: On the dependence of
463 winter precipitation types on temperature, precipitation rate, and
464 associated features. *J. Appl. Meteor. Clim.*, **49**, 1429-1442.
465 Thériaux, J.M. and R.E. Stewart, 2010: A parameterization of the microphysical
466 processes forming many types of winter precipitation. *J. Atmos. Sci.*, **67**,
467 1492-1508.

468 Thompson, G., R.M. Rasmussen, and K. Manning, 2004: Explicit forecasts of
469 winter precipitation using an improved bulk microphysics scheme. Part I:
470 Description and sensitivity analysis. *Mon. Wea. Rev.,* **132**, 519–542.
471 Thompson, G., P.R. Field, R.M. Rasmussen, and W.D. Hall, 2008: Explicit
472 forecasts of winter precipitation using an improved bulk microphysics
473 scheme. Part II: Implementation of a new snow parameterization. *Mon.*
474 *Wea. Rev.*, **136**, 5095-5115.
475 Thompson, G., and T. Eidhammer, 2014: A study of aerosol impacts on clouds
476 and precipitation development in a large winter cyclone. *J. Atmos. Sci.*,
477 **71**, 3636-3658. doi: http://dx.doi.org/10.1175/JAS-D-13-0305.1.
478 Vislocky, R. L., and G. S. Young, 1989: The use of perfect prog forecasts to
479 improve model output statistics forecasts of precipitation probability. *Wea.*
480 *Forecasting,* **4**, 202–209.
481 Wagner, A. J., 1957: Mean temperature from 1000 to 500 mb as a predictor of
482 precipitation type. *Bull. Amer. Meteor. Soc.*, **10,** 584-590.
483 Wandishin, M.S., M.E. Baldwin, S.L. Mullen, and J.V. Cortinas Jr., 2005: Short-
484 range ensemble forecasts of precipitation type. *Wea. Forecasting,* **20**,
485 609-626.

FIGURE CAPTIONS

Figure 1. Flowchart describing the diagnostic logic for determination of precipitation type. (Bold letters in tan boxes: (FZ, IP, R, S) = (freezing rain, ice pellets, rain, snow). Ptot, ptot-rs and psnow are the total, rain plus snow only (no graupel), and snow only (water-equivalent) precipitation, respectively, 1h indicating over the last hour. Prate is the instantaneous fall rate for different hydrometeor types (r – rain, s – snow, g – graupel). The maximum rain mixing ratio in the column is represented by Max(qr).

Figure 2. Precipitation type (colored hatched lines: snow - blue horizontal, rain – green vertical, freezing rain – red sloping upward to right, ice pellets – lavender sloping downward to right) from a 1-h forecast from an experimental version of the Rapid Refresh (RAP) using the explicit diagnostic method. The RAP 1-h forecast is valid at 1600 UTC 1 January 2015 and was initialized at 1500 UTC, 1 h earlier. Accumulation (inches; shading) is shown in top figure but not on bottom. Note that precipitation type is indicated for areas with 1-h precipitation (water equivalent) less than 0.01 in (0.25 mm) since p-type can be diagnosed with 1-h precipitation as low as 0.0001 mm. Circles shown are for major airports. a) Without any total 1-h precipitation. b) With total 1-h precipitation (water equivalent) in inches.

506

507 **Figure 3.** Same as Fig. 2 but with precipitation-type forecasts shown separately
508 for each p-type with rain (upper left), snow (upper right), freezing rain (lower left),
509 and ice pellets (lower right).

510 **Figure 4.** Surface present weather observations including precipitation type
511 valid at 1500 (top) and1600 UTC (bottom) 1 January 2015, courtesy of Plymouth
512 State University (http://vortex.plymouth.edu/myo/sfc/pltmap-a.html). Weather
513 symbols are described in http://www.meteor.wisc.edu/~hopkins/aos100/sfc-
514 anl.htm .

515 **Figure 5.** Same as Fig. 3, but for areas of non-zero 1-h precipitation in the form
516 of rain, snow, and graupel.

517
518 **Figure 6**. Same as Fig. 2 but using the dominant p-type diagnostic (Manikin
519 2005) combining Baldwin, Ramer, Bourgouin, and revised Baldwin diagnostics.

520

521 **Figure 7.** Sounding skew-T profile of temperature and moisture at Lubbock, TX,
522 for 1-h RAP forecast valid at 1600 UTC, same RAP run shown in Figs. 2 and 5.

523

524 **Figure 8.** Probability of detection for 4 different precipitation types, rain (red),
525 snow (blue), freezing rain/drizzle (orange), ice pellets (gray) from 1-h forecasts
526 from the ESRL experimental 13-km Rapid Refresh as verified against METAR
527 observations vs. nearest single 13-km grid points. Results are averaged over 30-

528 day periods including 2 winters over the period from August 2013 through 15
529 December 2015.

530
531 **Figure 9**. Same as Fig. 8 but for False Alarm Ratio. The explicit p-type is
532 applied for 1-h precipitation as low as 0.0001 mm/h to capture very light freezing
533 precipitation whereas METAR observation precision is limited to a minimum of
534 0.25 mm/h.

535 **Figure 10**. Same as Fig. 9 (False Alarm Ratio) but for 1-h total precipitation of at
536 least 0.01 inches/h (0.25 mm/h). Values are for 60-day averages.

537

538

539

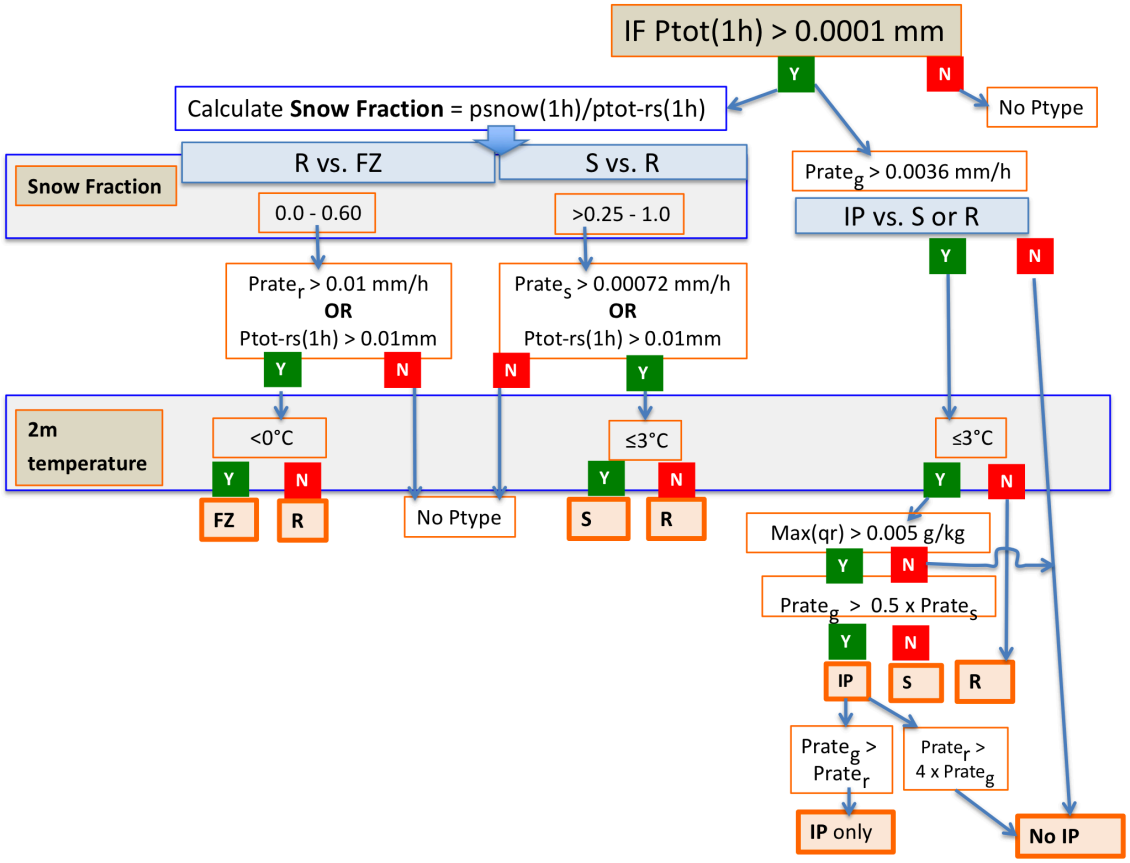

Figure 1. Flowchart describing the diagnostic logic for determination of precipitation type. (Bold letters in tan boxes: (FZ, IP, R, S) = (freezing rain, ice pellets, rain, snow). Ptot, ptot-rs and psnow are the total, rain plus snow (no graupel), and snow only (water-equivalent) precipitation, respectively, 1h indicating over the last hour. Prate is the instantaneous fall rate for different hydrometeor types (r – rain, s – snow, g – graupel). The maximum rain mixing ratio in the column is represented by Max(qr).

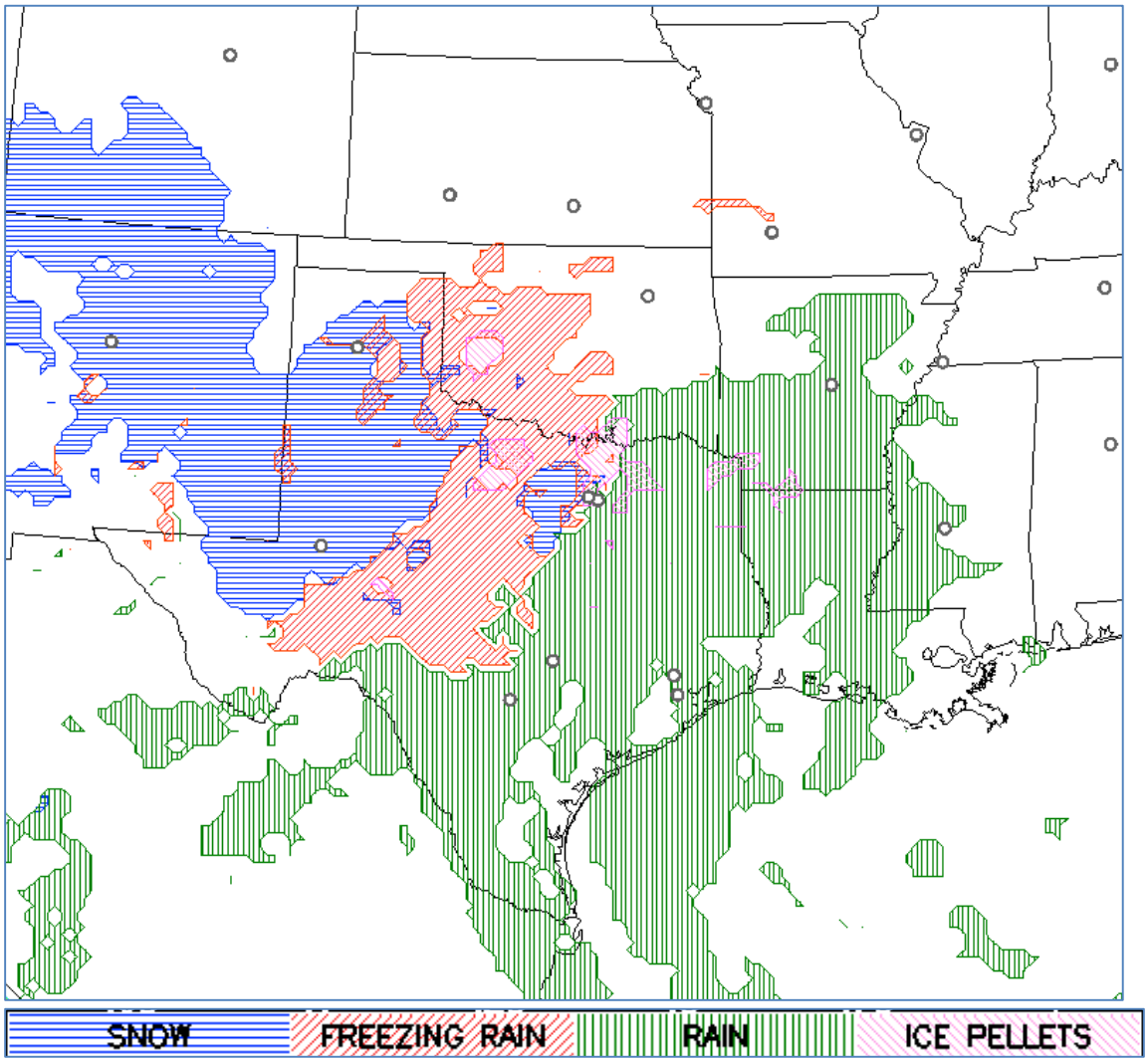

2a)

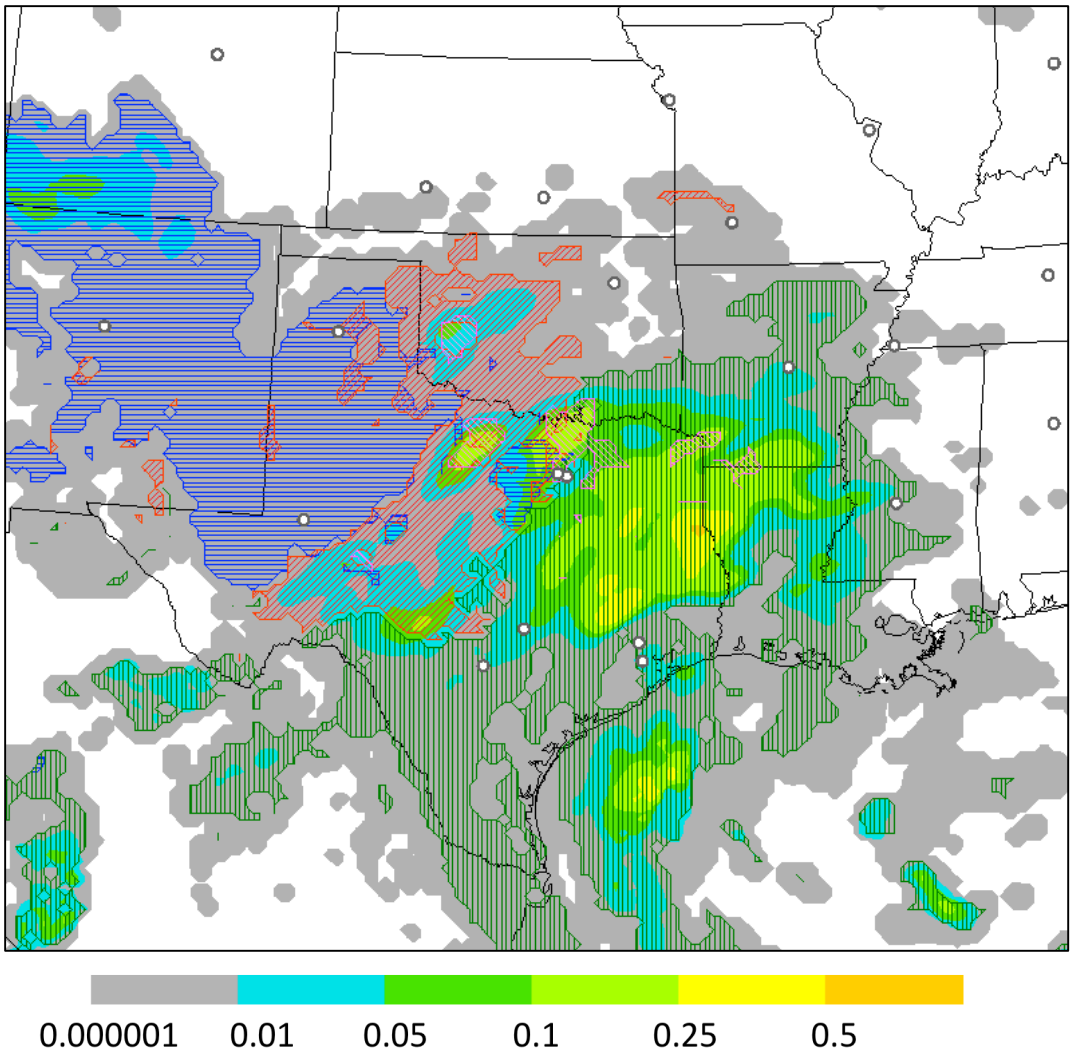

2b)

Figure 2. Precipitation type (colored hatched lines: snow - blue horizontal, rain – green vertical, freezing rain – red sloping upward to right, ice pellets – lavender sloping downward to right) from a 1-h forecast from an experimental version of the Rapid Refresh (RAP) using the explicit diagnostic method. The RAP 1-h forecast is valid at 1600 UTC 1 January 2015 and was initialized at 1500 UTC, 1 h earlier. Accumulation (inches; shading) is shown in top figure but not on bottom. Note that precipitation type is indicated for areas with 1-h precipitation (water equivalent) less than 0.01 in (0.25 mm) since p-type can be diagnosed with 1-h precipitation as low as 0.0001 mm. Circles shown are for major airports. a) Without any total 1-h precipitation. b) With total 1-h precipitation (water equivalent) in inches.

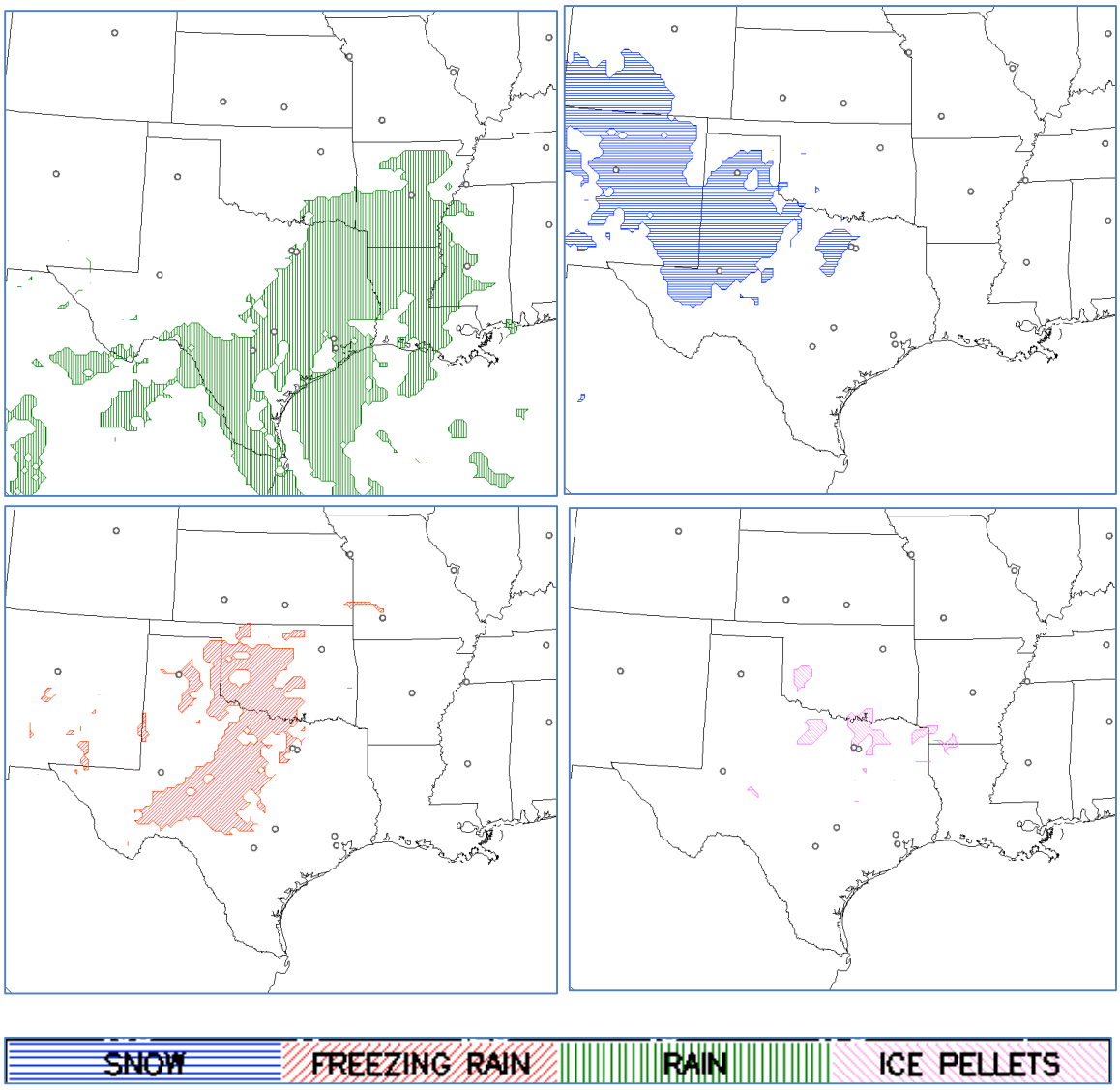

Figure 3. Same as Fig. 2 but with precipitation-type forecasts shown separately for each p-type with rain (upper left), snow (upper right), freezing rain (lower left), and ice pellets (lower right).

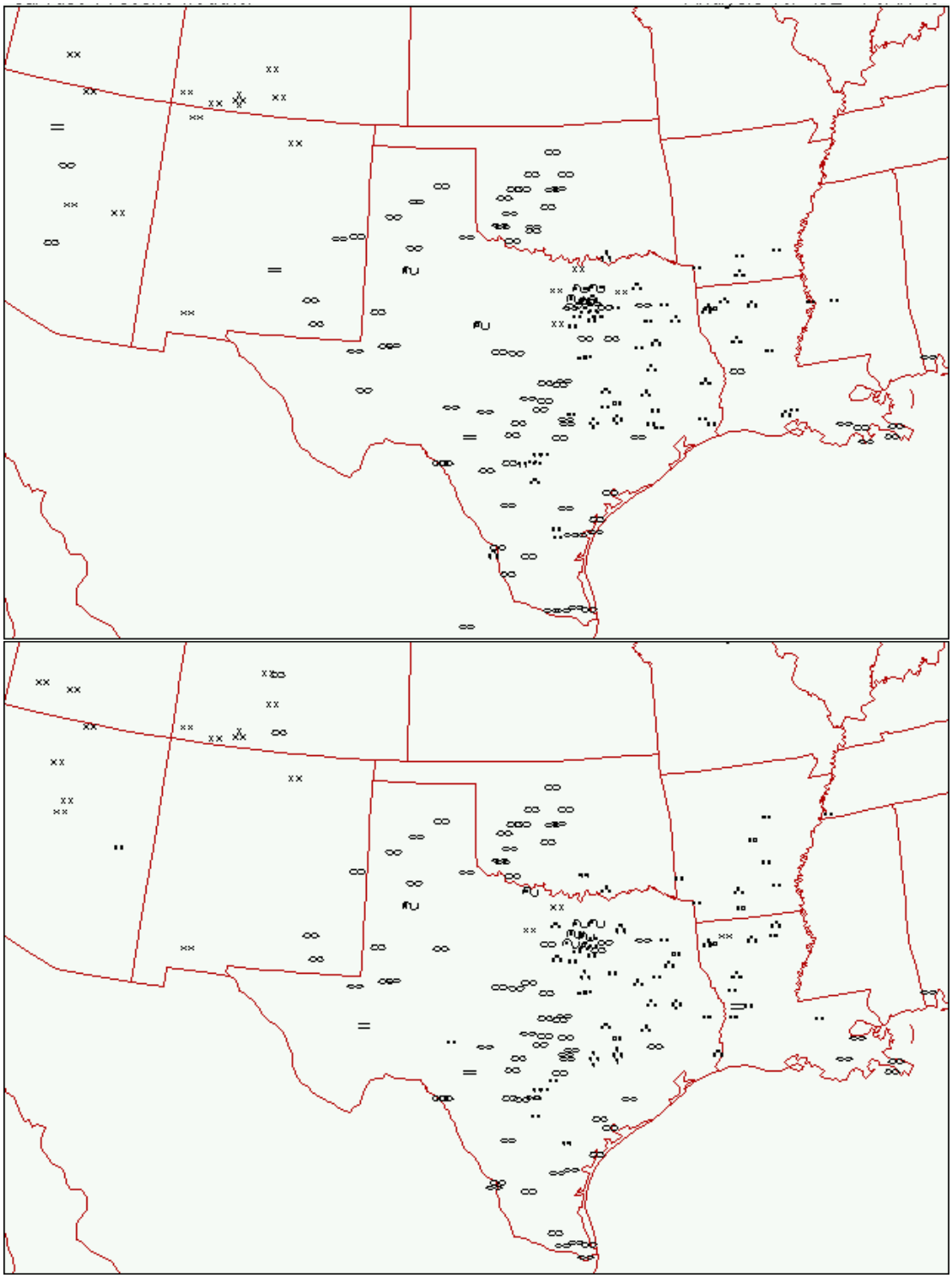

Figure 4. Surface present weather observations including precipitation type valid at 1500 (top) and 1600 UTC (bottom) 1 January 2015, courtesy of Plymouth State University (http://vortex.plymouth.edu/myo/sfc/pltmap-a.html). Weather symbols are described in http://www.meteor.wisc.edu/~hopkins/aos100/sfc-anl.htm.

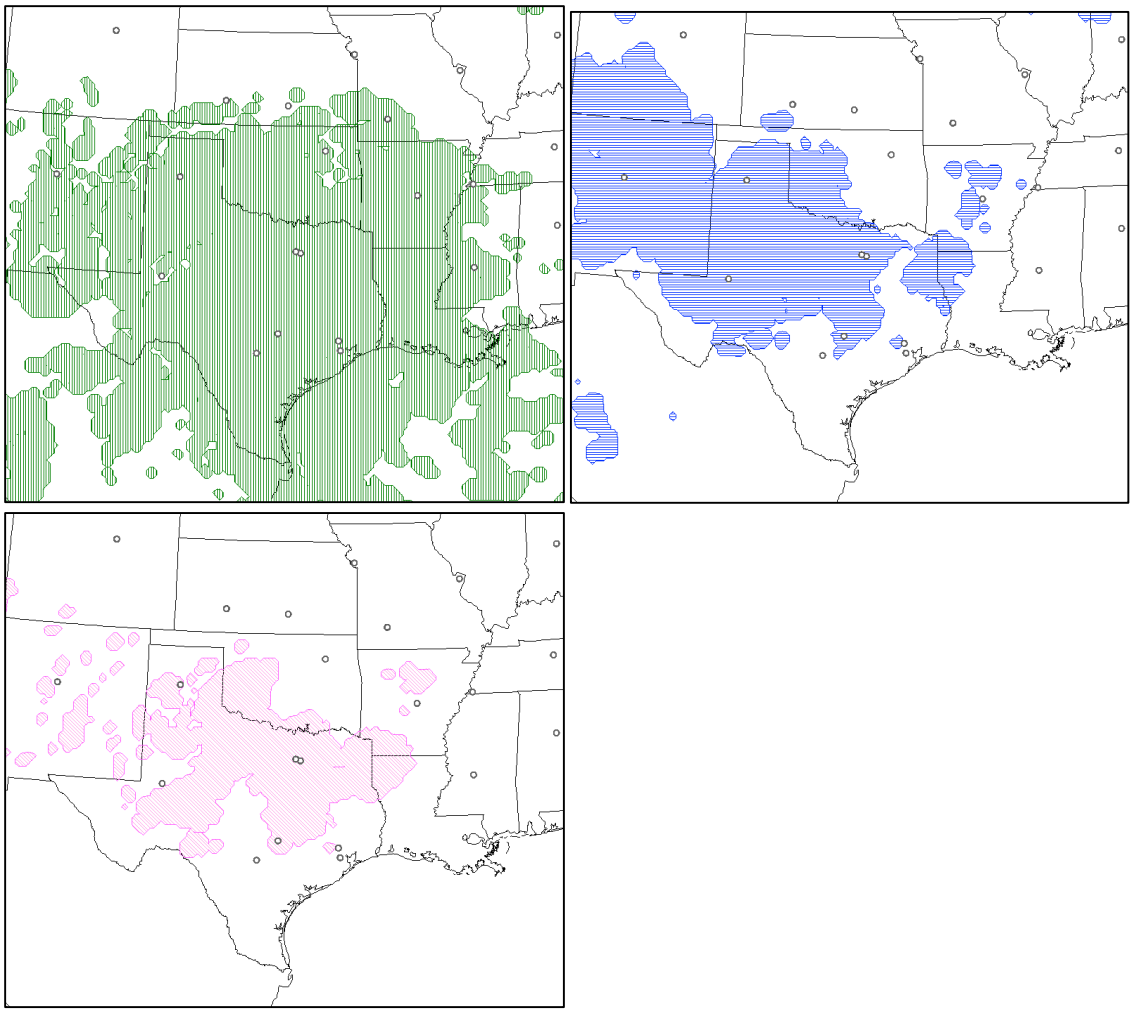

Figure 5. Same as Fig. 3, but for areas of non-zero 1-h precipitation in the form of rain, snow, and graupel.

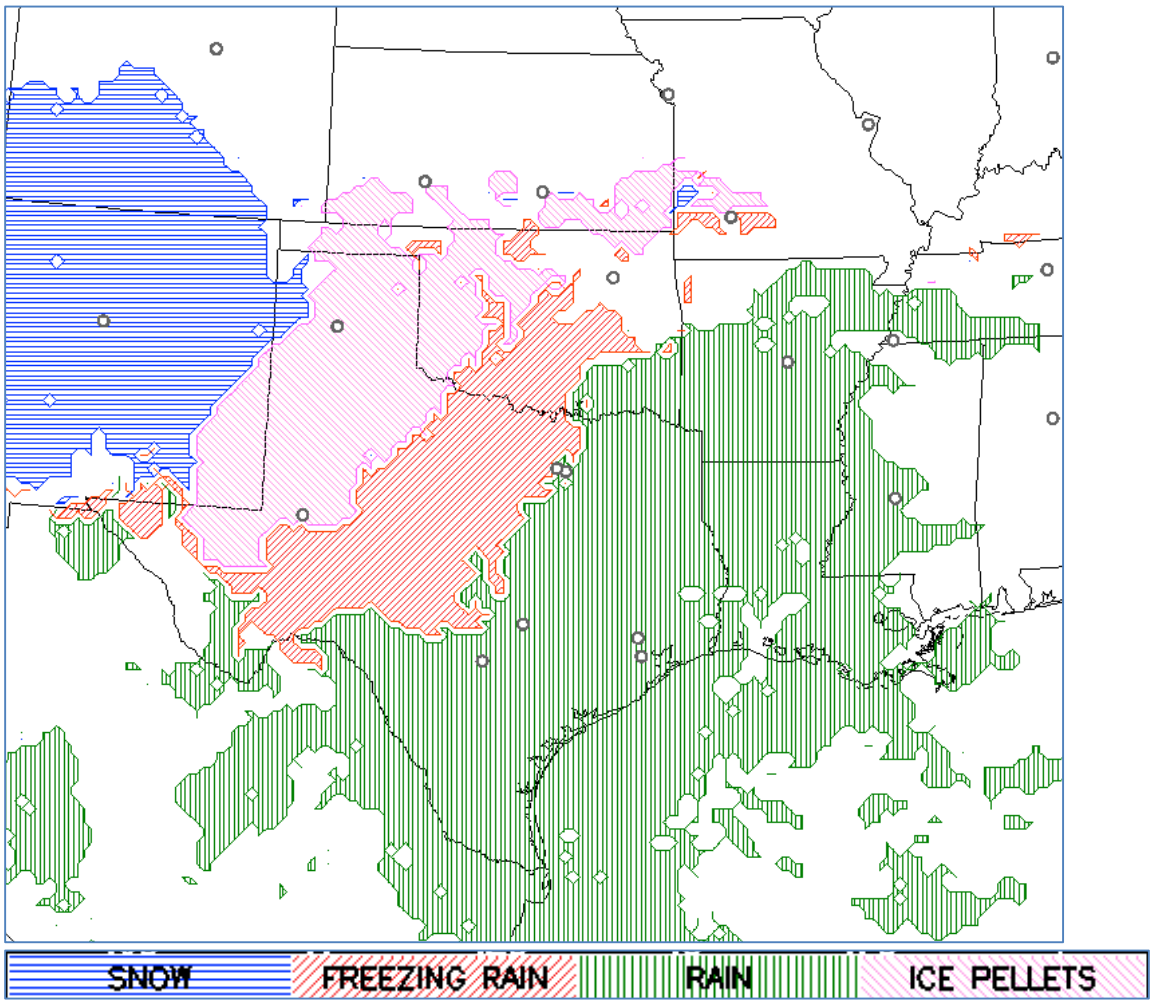

Figure 6. Same as Fig. 2 but using the dominant p-type diagnostic (Manikin 2005) combining Baldwin, Ramer, Bourgouin, and revised Baldwin diagnostics.

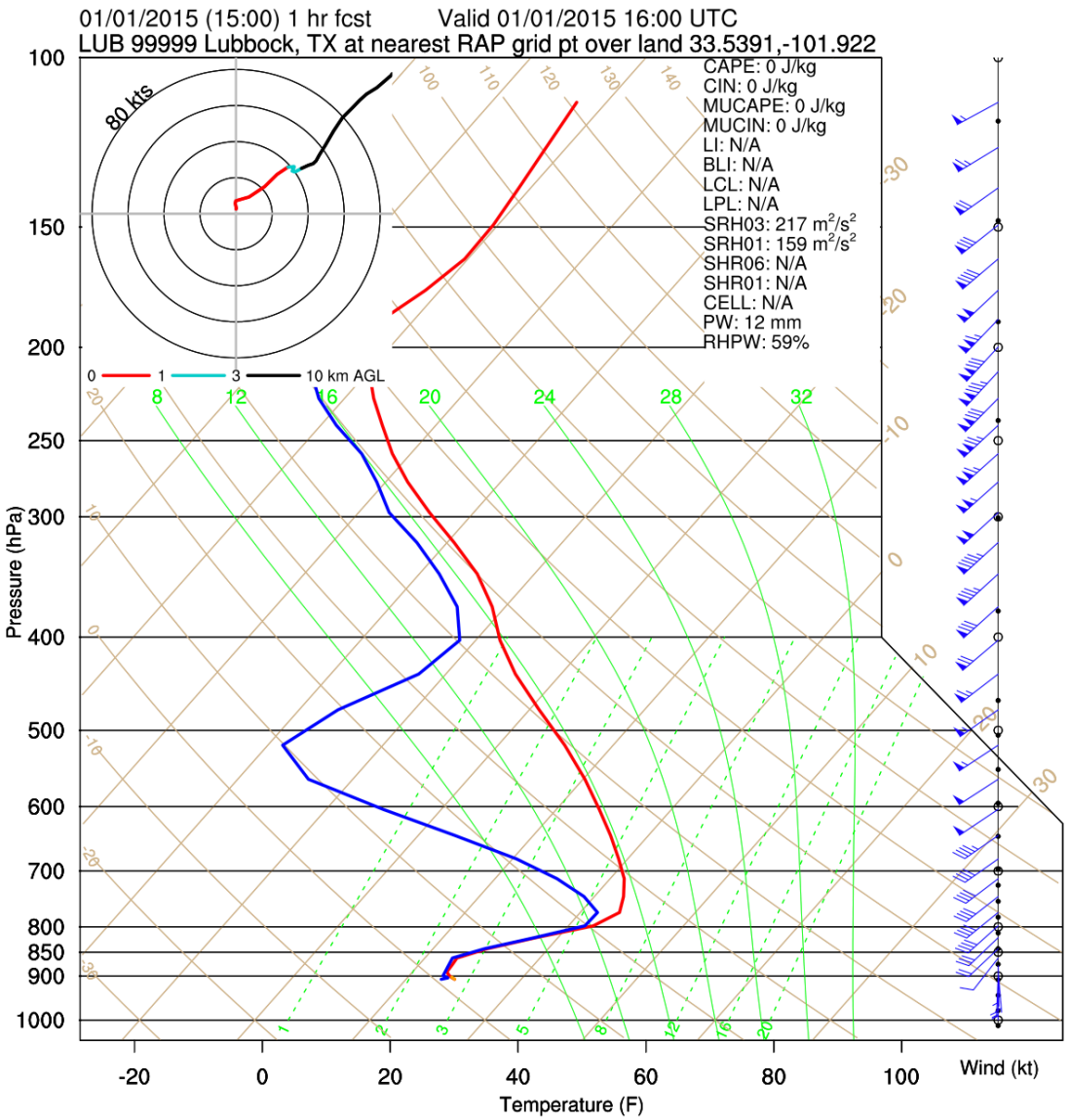

Figure 7. Sounding skew-T profile of temperature and moisture at Lubbock, TX, for 1-h RAP forecast valid at 1600 UTC, same RAP run shown in Figs. 2 and 5.

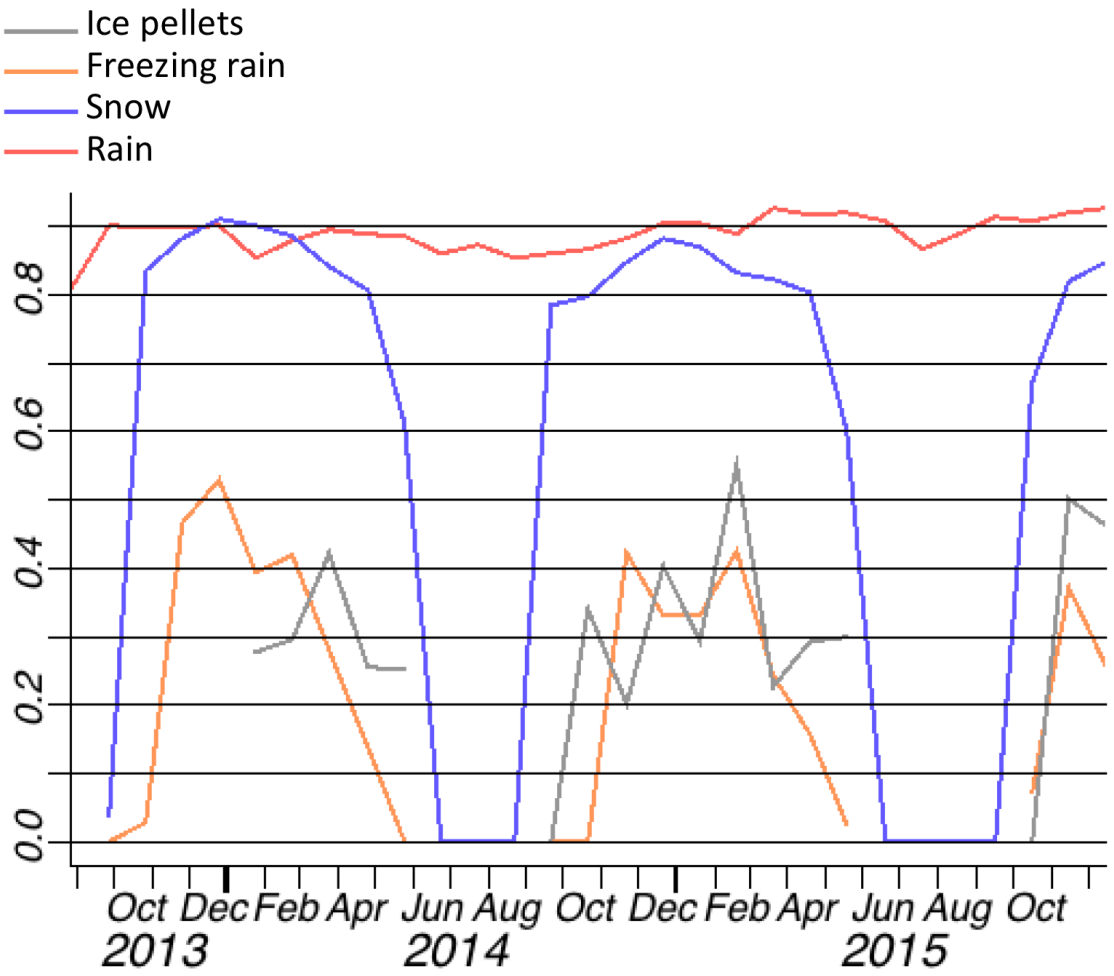

Figure 8. Probability of detection for 4 different precipitation types, rain (red), snow (blue), freezing rain/drizzle (orange), ice pellets (gray) from 1-h forecasts from the ESRL experimental 13-km Rapid Refresh as verified against METAR observations vs. nearest single 13-km grid points. Results are averaged over 30-day periods including 2 winters over the period from August 2013 through 15 December 2015.

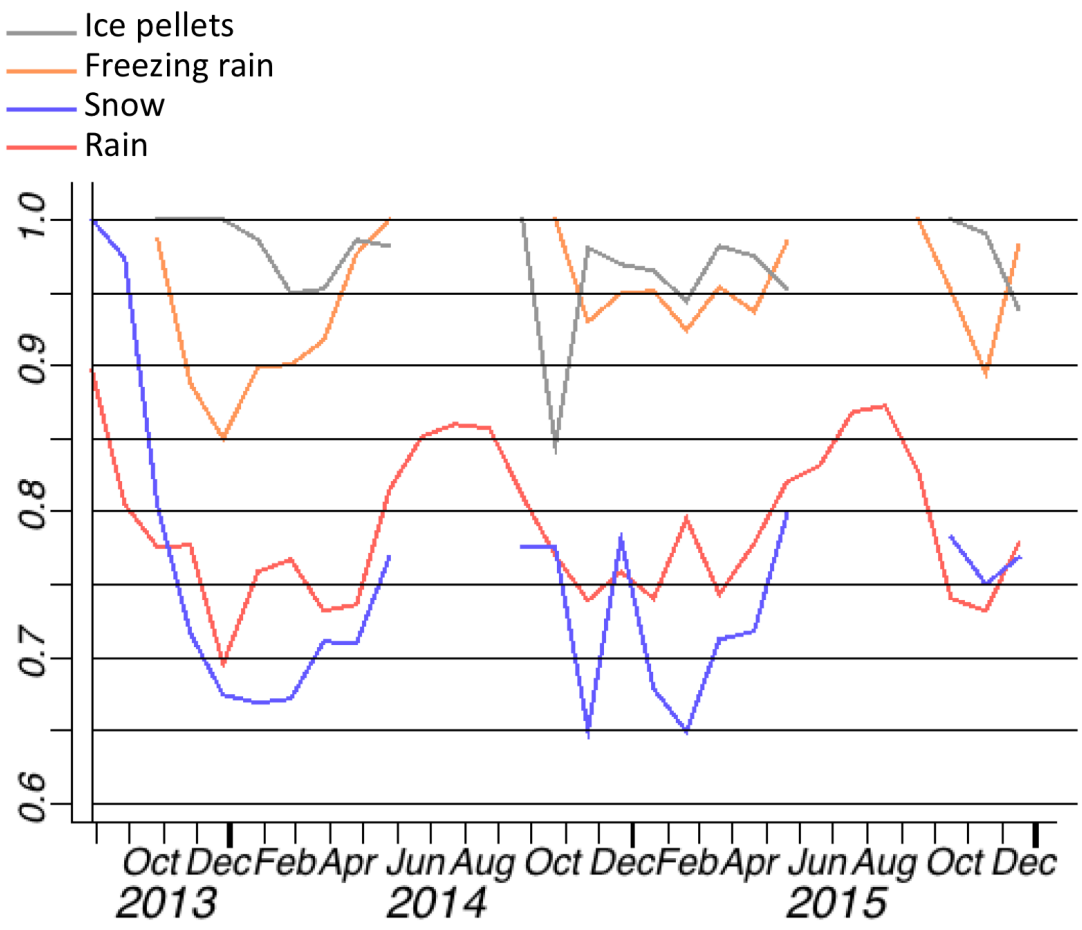

Figure 9. Same as Fig. 8 but for False Alarm Ratio. The explicit p-type is applied for 1-h precipitation as low as 0.0001 mm/h to capture very light freezing precipitation whereas METAR observations are limited to a minimum of 0.25 mm/h.

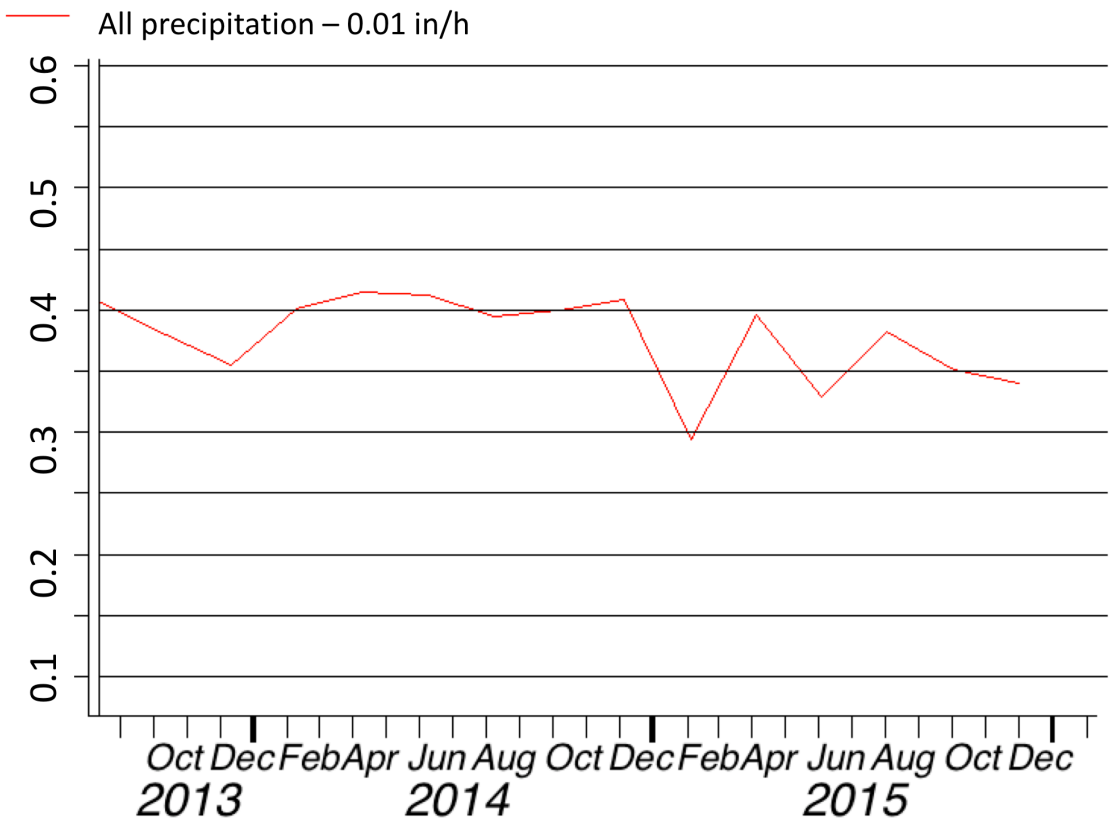

Figure 10. Same as Fig. 9 (False Alarm Ratio) but for 1-h total precipitation of at least 0.01 inches/h (0.25 mm/h). Values are for 60-day averages.